CR-124827

SPECTROGRAPHIC INVESTIGATION OF A SHOCK EXCITED ABLATION MATERIAL

By

Roger D. Bengtson

Thesis submitted to the Graduate Faculty of the

Virginia Polytechnic Institute

in candidacy for the degree of

MASTER OF SCIENCE

in

Physics

May 1964

SPECTROGRAPHIC INVESTIGATION OF A SHOCK EXCITED ABLATION MATERIAL

by

Roger D. Bengtson

Thesis submitted to the Graduate Faculty of the

Virginia Polytechnic Institute

in candidacy for the degree of

MASTER OF SCIENCE

in

PHYSICS

May 1964

Blacksburg, Virginia

II. TABLE OF CONTENTS

CHAPTER		PAGE
I.	TITLE	1
II.	TABLE OF CONTENTS	2
III.	LIST OF FIGURES	3
VI.	INTRODUCTION	4
V.	SYMBOLS	6
VI.	REVIEW OF LITERATURE	7
VII.	PRELIMINARY INVESTIGATION	11
VIII.	OPERATION OF THE SHOCK TUBE	13
IX.	DESCRIPTION OF EQUIPMENT	20
X.	OPERATING PROCEDURES	24
XI.	RESULTS	27
XII.	CONCLUDING REMARKS	31
XIII.	ACKNOWLEDGMENTS	33
XIV.	BIBLIOGRAPHY	34
XV.	VITA	39

III. LIST OF FIGURES

FIGURE		PAGE
1.	Equilibrium Gas Composition of an Elemental Mixture of 0.99 A, 0.006 H, 0.002 C, 0.001 Si, and 0.001 O	40
2.	Ideal Wave Motion in a Simple Shock Tube	44
3.	Schematic of a Normal Shock With Gas Parameters Noted . .	45
4.	Ideal Wave Motion in a Buffered Shock Tube	46
5.	Schematic of Experimental Apparatus	47
6.	Diaphragm and Scribe	48
7.	Pressure and Intensity Record	49
8.	Raster Timer Output	51
9.	Optical Path of Spectrograph	52
10.	Run Conditions	53
11.	Shock Excited Spectra	54
12.	Shock Excited Spectra	58

IV. INTRODUCTION

Upon reentry into the atmosphere of the earth of any other planet a space vehicle is subjected to a severe heating load. This heat load is generally beyond that which can be withstood by effective structural materials. One way to cope with the situation is the use of an ablative material which is effective in insulating the structural material against heat while undergoing thermal degradation in reradiating the incident radiation, and in absorbing energy. Ablative materials are applied to the exterior of temperature sensitive structures and materials to isolate them from the effects of their high temperature environment. Interaction with the high temperature environment produces a controlled erosion of the surface. The energy absorption processes which take place during the ablation of material from the surface reduce the surface temperature of the vehicle and greatly restrict the flow of heat into the vehicle structure.

The ablation of materials in high temperature environments is a subject of great complexity. Initially the heat incident upon the surface of an ablating heat shield is absorbed and conducted into the material. The heat penetrates at a low rate due to the low thermal conductivity of most ablative materials. Thus, the surface temperature of the ablator rises rapidly until thermal degradation begins. Many ablators form a char residue on the surface. With the formation of this layer of residue, the primary region of thermal degradation gradually shifts from the char surface to the interior of the material beneath the char. The newly formed char structure remains attached to the underlying virgin

material and is retained there. The refractory nature of this char protects the temperature sensitive material from the high temperature environment by reradiating a large portion of the radiative heat. Gaseous products formed by the pyrolysis of the ablative material move through the char layer and undergo a breakdown to lower molecular weight products which are injected into the adjacent boundary layer. Each phase of the overall process of ablation contributes to the overall protection provided by heat-shield material.

A complete theoretical analysis with a particular ablator material is impossible because of the many unknowns involved, and the great complexity of the various processes which are carried out. The present investigation has been carried out as a step in the effort to evaluate the behavior of an ablator material in an equilibrium high temperature environment. A powdered ablative material was placed in a shock tube and observed spectrographically in the visible and near ultraviolet regions of the spectrum as the material was exposed to the high temperatures behind a reflected shock. The spectra were then analyzed to determine the products of ablation. A correlation between environment temperature and thermal degradation of the ablative polymer was desired. The ablator material tested was the silicone polymer Sylgard 182 manufactured by Dow Corning. It has the chemical form

$$\left[\begin{array}{c} CH_3 \\ | \\ Si - O \\ | \\ CH_3 \end{array}\right]_n$$

V. SYMBOLS

a	speed of sound
F	free energy
h	enthalpy
I	intensity
M_S	shock Mach number
M_R	reflected shock Mach number
p	pressure
R	gas constant
T	temperature $^{\circ}K$
V	velocity
ρ	density
γ	specific heat ratio

VI. REVIEW OF LITERATURE

Since this work is a combination of hydrodynamics and spectroscopy, it is felt that it would be worthwhile to discuss developments in both areas. Vielle was the first to demonstrate the effectiveness of the shock tube as a research tool in 1899. The present phase of interest in the shock tube began with the second world war. The shock tube was used initially as an intermittent supersonic wind tunnel for aerodynamic testing. Later developments made it possible to use the shock tube to generate hypersonic flow (ref. 12). The shock tube was also used to study real gas effects in a hot gas moving at a high speed (ref. 33). Glass and Hall give a detailed bibliography to the experimental and theoretical papers and reports concerning shock tubes up to 1958 (ref. 11). At present the shock tube is used to study nonequilibrium phenomena in hypersonic flight (ref. 7), heat transfer measurements (ref. 36), chemical reactions and reaction rates (ref. 10), and boundary layer effects (ref. 18).

From a spectroscopic point of view, the high temperature of the gas behind the shock front in a shock tube provides an extremely powerful facility with which to excite luminosity either in the gas itself or in the matter with which it interacts. Spectroscopic analysis of the luminosity has both aided aerodynamic research and contributed to our knowledge of the chemical physics of hot gases and to atomic and molecular spectroscopy. The shock tube can be compared at least qualitatively to other more conventional spectroscopic sources such as furnaces, arcs,

flames, stars, and discharge tubes. The diatomic band systems of C_2 Swan, CN violet, CN red, CH, and OH, usually produced in arcs and furnaces as well as observed in astronomical sources have been excited in emission and absorption by the passage of shock waves through gaseous hydrocarbons. The spectra closely resemble those produced in flames (refs. 8 and 9). Numerous observations have been made on the molecular spectra produced in emission by the shock excitation of air, oxygen, and nitrogen. In this work, bands of the N_2 first and second positive system, the NOγ system and the O_2 Schumann-Runge system are prominent (refs. 14, and 38). Quantitative as well as qualitative observations have been made. Experiments by Wurster, Glick, and Treanor in absorption through shock heated air and oxygen have extended the O_2 Schumann-Runge system to include the (0,13) and (0,14) bands and have also given an integrated absorption coefficient from 2600 Å to 2900 Å for O_2 (ref. 39). Keck, Camm, Kivel, and Wentink have reported effective electronic f-numbers for the bands of O_2 Schumann-Runge, NOβ, NOγ, N_2 second positive, N_2 first positive, and N_2^+ first negative as a result of the shock excitation of oxygen, nitrogen, and air (ref. 15). Doherty used the shock tube as a source for the measurement of absolute spectral line strengths (ref. 6). Wilkerson used the shock tube for the measurement of gf-values for lines of neutral and singly ionized chromium (ref. 35). The f-number for the (0,0)-band of the $OH\ ^2\Sigma \rightarrow {}^2\Pi$ transition was measured by Lapp (ref. 17). Shackleford studied the spectrum of Ti I which was emitted behind reflected shock waves in $TiCl_4$-Ar mixtures (ref. 32). High temperature atomic spectra

arising from shock excitation of argon have been reported (ref. 30). Line broadening and shift as a result of the Stark effect have been observed for the hydrogen Balmer lines as a result of the high electron and ion density behind the shock wave (ref. 34).

The temperature of the hot gas behind the incident shock over a range from 2000° K to 8000° K has been measured by using the sodium-line reversal method (ref. 5). Spectrographic rotational temperature measurement on the (0,1)-band of the CN violet system has provided a means of inferring a temperature without introducing temperature sensitive devices such as probes into the environment (refs. 26 and 27).

Much of the work in shock tube spectroscopy has been mainly concerned with the excitation of spectra by the passage of shock waves through gases, but there have been complementary studies upon a number of aspects of the interaction of shock waves with a powdered solid. A wide range of inorganic oxides, nitrides, hydrides, carbides, and sulfides have been treated by this method. Parkinson and Reeves investigated the band systems of TiO, TiN, and BeO (ref. 28). The emission spectra of powdered meteorite samples after interaction with a strong shock were compared with those of meteors taken in flight (ref. 25). There was excellent agreement in the shock excited spectra of meteorite specimens studied with the atomic features reported in meteor spectra. This agreement is interesting when it is recalled that meteor spectra from periodic meteors arise from the powder ablation from small fragile porous solids. The spectra from several shock excited organic aromatic compounds were studied by Nicholls,

Parkinson, and Reeves (ref. 23). The main features of these spectra were C_2, CN, and CH. No atomic features other than impurities were noted in the spectra of shock excited organic compounds. The technique of the excitation of spectra by the interaction of a shock wave and a powdered solid shows promise of becoming a strong tool in the field of spectroscopy.

VII. PRELIMINARY INVESTIGATION

The Structures Research Division at Langley Research Center has undertaken studies of the thermal degradation on the silicone polymer Sylgard 182. The polymer was thermally degraded by heating it with a small platinum coil. The decomposition took place in an inert helium atmosphere. The temperature was in the range of 1000° C. The gaseous products formed were analyzed by a time of flight mass spectrometer after separation by a gas chromatograph. The results show that Sylgard 182 degrades thermally into methane and a series of cyclic silicones.

An analytic investigation was conducted as a part of this thesis to determine the equilibrium chemical composition of a mixture of gases usually found in a typical shock tube run behind the reflected shock after the ablator material had completely decomposed into a gas.

The elemental composition considered was made up of 0.99 mole fraction argon, 0.006 mole fraction hydrogen, 0.002 mole fraction carbon, 0.001 mole fraction silicon, and 0.001 mole fraction oxygen. This composition would not be an unreasonable estimate of the conditions encountered behind the reflected shock in the shock tube although the figure of 0.99 mole fraction of argon is probably too small. The chemical species which were considered were A, C, C_2, C_3, C_2H_2, CO, H, H_2, O, Si, Si_2, SiH, SiO, CH, CH_2, CH_3, CH_4, C_2H_4, CO_2, HCO, H_2O, O_2, OH, SiH_4, and SiO_2.

This investigation used a general IBM 704 or 7090 computer program for the computation of chemical equilibrium compositions developed by

Zeleznik and Gordon. This program uses an iterative technique to solve the equations for the equilibrium conditions. The condition of chemical equilibrium is that the free energy change across a chemical reaction at a constant temperature and pressure is equal to zero

$$\Delta F_{\text{any reaction}} = 0$$

This criteria for equilibrium requires that the equilibrium constant be known for each independent reaction considered. Then at a given pressure and temperature, the composition of a reacting equilibrium system can be calculated if the initial composition is known. In the method of solution used in the IBM program, the nonlinear set of equations developed from the equilibrium constants and the desired pressure and temperature were replaced by a set of linear equations obtained by a Taylor series expansion which neglects terms higher than the first order. The equilibrium compositions were then obtained by a Newton-Raphson iteration. See references 40 and 41 for a description of the program and the methods used in determining the equilibrium composition. Equilibrium conditions were calculated for the temperature range of 3000° K to 6250° K and pressure range of 1 atmosphere to 5 atmospheres. The program could be used only to the temperature of 6250° K. The results of this investigation are shown in figure 1.

VIII. OPERATION OF THE SHOCK TUBE

A shock wave is a sharp transition zone between two thermodynamic states in a compressible medium. A shock appears whenever a disturbance in the medium becomes so large that the sonic (acoustic) waves cannot dissipate the energy before the disturbed region expands by mass motion. A shock is formed only by the compression of gases, and not by an expansion of a gas. The gas passes through the shock and suffers rapid pressure and density increases which are generally much larger than those encountered in acoustic waves. Explosions and fluid flow past objects at supersonic speeds are common ways of creating shocks, but the simplest shock phenomena is the plane wave produced in the shock tube, which is a straight pipe of constant cross section. Many different types of shock tubes are in use today, but the basis of operation is similar for all.

A simple shock tube consists of a cylinder of constant cross section and divided into two sections by a gas-tight diaphragm. The first section, the driver chamber, contains a gas at a high pressure, p_4, and the second section contains the test gas at a low pressure, p_1, where $p_4 \gg p_1$. When the diaphragm separating the two sections breaks, a shock wave travels into the driven section at a supersonic velocity. The compressed gas behind the shock wave provides a high speed flow for aerodynamic studies. When the shock wave reaches the end of the tube, it undergoes a reflection to satisfy the boundary condition of $\bar{V} = 0$ at the wall. This stationary sample of gas is now at a high pressure and high temperature and may be self-luminous. Figure 2 shows the ideal wave motion in a shock tube.

A complete theory of shock tube flow can be constructed under the assumption that the gases are inviscid and undergo one-dimensional motion. It is necessary to measure only the velocity of the shock wave as it progresses down the tube and the pressure and temperature of the gas in front of the shock to predict the temperature and pressure behind the normal shock. It is assumed that the speed of sound of the gas in the test section is known. Consider the schematic drawing of a normal shock shown in figure 3. The conditions across the shock must satisfy the three conservation equations where the coordinate system is centered at the shock

$$\rho_1 V_1 = \rho_2 V_2 \qquad \text{mass}$$

$$h_1 + \frac{1}{2} V_1^2 = h_2 + \frac{1}{2} V_2^2 \qquad \text{energy}$$

$$p_1 + \rho_1 V_1^2 = p_2 + \rho_2 V_2^2 \qquad \text{momentum}$$

and an equation of state for a perfect gas

$$p = \rho R T$$

From these equations the following fundamental shock formulas in laboratory coordinates in terms of shock Mach number can be derived:

$$\frac{V_2}{V_s} = \frac{2}{\gamma + 1}\left(\frac{M_s^2 - 1}{M_s}\right)$$

$$\frac{\rho_2}{\rho_1} = \frac{\gamma + 1}{\gamma - 1}\left(\frac{M_s}{M_s^2 + 2}\right)$$

$$\frac{p_2}{p_1} = \frac{2\gamma M_s^2 - (\gamma_1 - 1)}{\gamma + 1}$$

$$\frac{a_2^2}{a_1^2} = \frac{T_2}{T_1} = \frac{\left[2\gamma M_s^2 - (\gamma - 1)\right]\left[(\gamma - 1)M_s^2 + 2\right]}{(\gamma + 1)^2 M_s^2}$$

where the Mach number M is defined as

$$M = \frac{V_s}{a} = \frac{\text{Shock velocity}}{\text{Speed of sound}}$$

and where the shock velocity is relative to the gas into which it is moving and the speed of sound is that of the gas into which the shock is moving.

The gas temperature after the incident shock wave can be further increased by reflecting the shock wave at the end of the tube as shown in figure 2. If a shock is reflected from the end wall of the tube, the gas temperature and pressure are increased and the gas is brought to rest. The reflected shock wave must produce an induced flow velocity in region 5 which is equal and opposite to $\bar{V}_2$ in order to bring the gas to rest

after the reflected shock. If V_R is the velocity of the reflected shock wave, the Mach number ahead of the shock wave is

$$M_R = \frac{V_2 - V_R}{a_2}$$

From the induced velocity after a moving normal shock wave relationship, the following equation is obtained:

$$\frac{V_2}{a_2} = \frac{2}{\gamma + 1}\left(M_R - \frac{1}{M_R}\right)$$

Since the left side of this equation is the flow Mach number after the incident shock wave, the reflected Mach number M_R can be determined as a function of the shock velocity and the state of the gas in region 1. The flow Mach number after the incident shock wave is given by

$$M_s = \frac{2(M_s^2 - 1)}{\sqrt{\left[\left\{2\gamma M_s^2 - (\gamma - 1)\right\}\left\{(\gamma - 1)M_s^2 + 2\right\}\right]}}$$

The pressure ratio behind the reflected shock wave is

$$\frac{p_5}{p_2} = 1 + \frac{2\gamma}{\gamma + 1}\left(M_R^2 - 1\right)$$

and the corresponding temperature ratio in the stagnant region is

$$\frac{T_5}{T_2} = \frac{\left\{2\gamma M_R^2 - (\gamma - 1)\right\}\left\{(\gamma - 1)M_R^2 + 2\right\}}{(\gamma + 1)^2(M_R^2)}$$

These ratios can also be used to find

$$\frac{T_5}{T_1} = \frac{T_5}{T_2} \cdot \frac{T_2}{T_1}; \quad \frac{P_5}{P_1} = \frac{P_5}{P_2} \cdot \frac{P_2}{P_1}$$

Thus, by measuring the velocity of the shock as it moves down the tube, and the pressure of the gas in the test section, one is able to predict the pressure and temperature of the gas behind the normal and reflected shocks. The presence of a boundary layer may alter the assumption of one-dimensional flow and consequently the conditions behind the reflected shock.

At high temperatures real gas effects come into play. The diatomic molecules will become excited, dissociate, ionize, and form chemical compounds. A monatomic gas becomes ionized at high temperatures. The perfect gas equation no longer holds, and it becomes necessary to use the real gas properties to determine the thermodynamic properties and composition of the gas. Tables of shock tube performance considering real gas effects for argon are shown in reference 1.

The shock tube used in this investigation was a modification of the simple shock tube. It is a cylinder with constant cross-sectional area divided into three sections by diaphragms and is generally referred to as a buffered shock tube. The use of a buffer section offers a convenient method of improving the shock tube performance. The first section, the driver chamber, contains a gas at a high pressure p_4. The middle or buffer section contains a gas at a low pressure p_1. The third section, the driven section, contains gas at a lower pressure p_{10} where

$p_4 \gg p_1 > p_{10}$. When the diaphragm separating the driver and buffer section breaks, a shock wave travels into the buffer section. It breaks the second diaphragm upon contact. Another shock then moves down the driven section at a high velocity. The ideal wave motion in a shock tube is shown in figure 4. The use of a buffered shock tube gives a higher Mach number for a given pressure ratio p_4/p_1 because the hot moving gas in the buffer section effectively becomes the driver for the gas in the driven section.

The shock tube has several strong features to recommend its use as a spectroscopic source. One of its most useful features is the fact that many different gases can be used as the test gas, and other materials may be placed in the gas to produce the atoms and molecules desired. Another advantage is that the excited gas is usually easily accessible to observation through windows or a transparent test section. A strong feature also is the fact that the gas is considered to be in thermal equilibrium and is at a relatively uniform temperature when compared to conventional spectrographic sources such as the arc or spark. Under usual test conditions, the density behind the reflected shock is sufficient to attain thermal equilibrium in much less than the test time. The temperature can be more accurately determined by aerodynamic calculations than the temperature of an arc or flame is known.

A disadvantage of the shock tube as a spectrographic source is its short run time. The usual run time is on the order of milliseconds with a maximum of perhaps 5 milliseconds. This means that a fast film and a spectrograph with large light gathering capability must be used to

view the short burst of illumination. Another disadvantage is the contamination from the walls, gas impurities, and heated diaphragm particles. Special cleaning precautions and shutter mechanisms are often used to cut down on the level of contamination in the shock tube spectra.

IX. DESCRIPTION OF EQUIPMENT

The experimental apparatus is shown schematically in figure 5. The driven section of the shock tube was made of 3.8-inch I.D. stainless steel seamless tubing 16 feet long. The test section was also made of stainless steel and is 14 inches long. The buffer section was made of 3.8-inch I.D. carbon steel seamless tubing 8-1/2 feet long. The driver section was made from carbon steel 3.8 inches in diameter and is 24 inches in length.

A stainless steel diaphragm 0.018 ±0.001 inch thick scribed with a narrow scribe so that 0.010 ±0.001 inch of material remained separated the buffer section from the driven section. Two stainless steel diaphragms 0.050 ±0.002 inch scribed so that 0.032 ±0.002 inch of material remained were used to separate the buffer section from the driver section. A 3-inch spacer separated the two diaphragms at the driver. All diaphragms were scribed with a circular tool to reduce stress concentrations at a point. Figure 6 shows a detail of the disphragm and scribe.

Argon was used as a test gas because of its chemical inertness and high molecular weight. Air was used in the buffer and driver sections since it gave the desired shock strengths.

The shock heated gas was observed through a 2-inch-diameter fused quartz window at the end of the test section. It was found that the spectra obtained looking along the shock tube axis had less contamination than the spectra obtained looking in a side window across the shock tube because of boundary layer effects. This is in agreement with results

obtained by Keck, Camm, Kivel, and Wentink (ref. 15). A fused quartz lens was used to focus the radiation from the test section onto the spectrograph slit. An electromagnetic shutter was used to limit the spectrograph exposure to less than 1.5 msec after the normal shock entered the test section. This shutter had an operation time of about 70 μsec from complete open to complete closing. The shutter used the electromagnetic force developed by the discharge of a 1-μf capacitor through a coil to collapse a thin foil. The use of the shutter reduced the contamination level on the spectrographic plates considerably by cutting out the radiation due to heated diaphragm particles coming down the tube after the useful run time. The figure of 1.5 msec for the shutter closing point mentioned earlier was chosen because of the length of the test time as shown by pressure records. The radiation intensity in the test section was viewed with a phototube through one of the side windows. This measurement gave a correlation between the pressure and intensity data. A sample output is shown in figure 7.

The initial pressure in the driven section was measured on a thermocouple gage calibrated in argon. The initial pressure in the buffer section and the high pressure in the driver section were measured on strain gage diaphragm type pressure transducers. The pressure measurement system for the absolute gas pressure behind the reflected shock consisted of a piezoelectric Kistler 6LM quartz transducer, and a Kistler charge amplifier used with a short time constant. The transducer was mounted in the wall of the test section 5 inches from the end of the test section. A force against the face of the quartz transducer was transmitted to the

internal prestressed quartz crystals and induced a charge across the electrodes attached to the crystals. A coaxial cable connected the electrodes to the charge amplifier which is used to match the high internal impedance of the transducer to that of the oscilloscope input and to convert charge to voltage. The high impedance of the quartz crystal enabled the system to be calibrated with static pressure. Figure 7 shows pressure record.

Shock speeds were measured by means of several ionization gaps which indicated shock arrival times by means of a spark breakdown across the gap as the shock passed by. The maximum sensitivity was achieved by setting the voltage across the ionization gap as high as possible without spontaneous triggering. The ionization gap output was recorded on an oscilloscope with a raster timer to yield the shock travel time. The raster timer was used to provide a better scale for the measurement of the shock arrival times. Figure 8 shows a sample output as taken from the oscilloscope. The velocity of the shock was assumed to be constant as it moved into the test section. The ionization gaps were also used to provide a trigger pulse for the electromagnetic shutter and to trigger the oscilloscope which recorded the pressure and intensity in the test section.

In order to study the short duration flash of luminosity a spectrograph of considerable light gathering power was necessary. An f/6.3 Jarrell Ash large aperture plane grating spectrograph which used a Fastie mounting was used to record the spectra. Figure 9 shows the optical path in this spectrograph. The spectrograph used a fixed slit of 40 microns in

width and 15 mm high. The use of any narrower slit reduced the intensity to an impractical level. The grating has a ruled area of 102 × 102 mm with 600 grooves/mm. The linear dispersion is 20.5 Å/mm in optimum position. The total wavelength range covered with each setting of the spectrograph was about 3000 Å, and all was in sharp focus. At the optimum position, the spectrograph can resolve lines that are 0.4 Å apart. Kodak 103-F and Kodak 103-0 plates were used because of their superior speed to record the shock excited spectra. A filter was mounted in front of the film plane to cut out second order spectra.

X. OPERATING PROCEDURES

The driven section of the shock tube was pumped down to about 10 microns before each run using a mechanical vacuum pump and a liquid nitrogen cold trap. Argon was bled in to approximately atmospheric pressure and the driven section again pumped down to 10 microns. Several minutes before the run argon was bled in to the desired operating pressure, usually about 20 mm Hg. The leak rate was low enough so that it did not affect the pressure of the argon in the driven section during the few minutes before the run. The driver and buffer sections were pumped down to about 1.5 mm Hg with a small vacuum pump. After the buffer section was pumped down, the pumps were isolated from the system and air was bled into the buffer section until the desired operating pressure was reached, usually on the order of 2 psi. After all the vacuum pumps were isolated and conditions fixed in the buffer and driven sections, the driver section was pressurized. The driver section was brought to a final pressure of 100 atmospheres of air. At the same time, the volume between the two diaphragms which separated the driver and buffer section was pressurized to 30 atmospheres with air. The pressure between the two diaphragms was suddenly lowered to atmospheric pressure through a small tube connected to the volume between the diaphragms causing both diaphragms to break. A shock wave then progressed down the tube.

The driven section and test section were cleaned between each run using a cloth soaked in trichloroethylene and then wiped with a clean

dry lint-free cloth. The use of an exacting cleaning procedure was found to be necessary to cut down the contamination in the spectra. The buffer section was cleaned with a cloth soaked in trichloroethylene.

The solid ablator material was powdered by using emery paper under liquid nitrogen to get the small particles. The material was cleaned in an acetone bath after being powdered to remove any foreign matter. The particle size ranged from 1/100 to 1/10,000 of an inch in diameter. The small particles tended to stick together making the value of any measurement of particle size rather doubtful.

Several methods were tried to position and hold the material in the tube. The best method found was to put the powder on a 1/2-inch-wide strip of Kleenex which was hung in the tube about a foot from the window. Vacuum grease was used to hold the Kleenex to the tube. The powder would not easily adhere to the Kleenex so it was necessary to put several drops of clean acetone on both the powder and the Kleenex. When the acetone evaporated, a thin film of powder was left on the surface. The acetone also tended to break apart the small particles. The Kleenex was placed in the test section so that the powder was on the upstream side. Several runs were made with only the piece of Kleenex with acetone on it in the tube to determine the effect of Kleenex and acetone on the contamination level of the spectra. The Na and Ca lines were the only impurities recorded from the Kleenex.

The spectrographic plates were developed in a completely darkened room in Kodak D-19 developer. The development time was as recommended by Kodak for the temperature of developer at the time. The plates were

washed in water before being fixed for 2 minutes in Kodak rapid fixer. Only one plate was developed in each batch of the developer and fixer solution.

The photographic density of the spectrographic plates was measured with a recording microdensitometer. The transmission of small film areas was measured by means of a photomultiplier which sets in the image plane of a microscope. The film lay in the object plane and was illuminated from behind by a steady light source. The film was moved at a uniform rate perpendicular to the optic axis, and the photomultiplier signal was simultaneously recorded on moving paper. The tracing then represented the variation of photographic density along the direction which the film is moved. These tracings were then used for a wavelength calibration of the plate.

XI. RESULTS

In the first experiments an effort was made to excite argon as a test gas. Since the Mach number used was always below 7, the intense luminosity produced behind the reflected shock was found to be due to the excitation of copper, iron, magnesium, calcium, sodium, titanium, and chromium from the walls of the tube. The lack of argon radiation was due to its resonance potential of 14.5 ev being much higher than the temperature in the tube. For example, Ca has a resonance potential of 5.0 ev. Repeated cleansing and polishing, continued use of the tube, and the use of an electromagnetic capping shutter reduced the impurities in the spectra so that they did not seriously hinder the analysis of the spectra.

Figure 10 shows the conditions for each run. There was a large discrepancy between the calculated pressure p_5 behind the shock and the measured pressure. This error was due to a boundary layer effect. Mark describes the interaction of a reflected shock wave with the boundary layer in a shock tube in reference 19. His analysis and results show that the pressure behind a reflected shock wave will be lower than that predicted by aerodynamic theory due to the interaction of the reflected shock wave and the boundary layer. The pressure drop behind the shock would become larger as the shock moved further away from the wall. This effect is shown on the sample output on figure 7. The gage was located 5 inches from the end of the test section. At this position, the boundary layer could have a large effect. Immediately after

reflection from the end wall the boundary layer effect is small. The boundary layer would also tend to lower the temperature behind the reflected shock. The spectrograph slit was focused at a point just inside the window so the initial conditions after the reflected shock could be determined by a one-dimensional flow analysis. An attempt was made to determine the rotational temperature from the (0,1)-band of the CN violet system as in reference 25, but the band structure was generally not well enough defined to make this a usable technique.

Figures 11(a) and 11(b) show the visible spectra from 3500 Å to 6500 Å in order of increasing temperature. Figure 11(b) also shows a run with just Kleenex. Figures 11(c) and 11(d) show the near ultraviolet spectrum from 2400 Å to 3400 Å also in order of increasing temperature. The identification of the excited lines and bands was made from references 20, 21, 22, and 29. The impurities in the shock tube served as a reference spectra so it was unnecessary to use any other reference such as an iron arc. Figure 12 shows a spectra with the lines identified and the wavelengths tabulated.

The spectra resulting from the decomposition of the Sylgard were C_2 Swan bands, C I, and SiI. The C I line was excited only at the highest temperature. The spectra of hydrogen, oxygen, carbon monoxide which might be expected to appear from the figures on equilibrium composition (fig. 1) were not seen because their excitation potentials are too high for the temperatures encountered in these tests.

At the lowest temperature at which tests were conducted (5000° K), the main features of the spectra were the C_2 Swan band, a few rather weak silicon lines and the CN bands with a continuous background. The continuous background was probably due to particles which were heated throughout before they vaporized and thus radiated much as a black body. The level of ionization was so low that the continuum could not have been due to free-free or free-bound electron transitions. Nicholls, Parkinson, and Reeves report a similar continuum in reference 23. The radiation from impurities was low at the low temperatures.

At the higher temperatures, the SiI lines became more prominent, the C_2 bands decreased in intensity slightly, and the CN bands became stronger. The level of radiation contamination was higher than at the lower temperature range. At the highest temperature tested the C_2 bands had nearly disappeared; a strong carbon line appeared at 2478.6 Å and the SiI lines became much stronger. The radiation due to impurities had also increased. The disappearance of the C_2 band system and the appearance of a strong carbon line is in excellent agreement with the data on equilibrium composition shown in figure 1. The CN bands were present in all runs despite the cleaning procedure and the pump-down procedure used. No attempt was made to account for the presence of CN in the spectra.

The ablative mechanism of the shock excited particles in the shock tube was not known. It seems most probable that passing through

the shock wave caused a molecular vapor to be evaporated. This molecular vapor, probably in the form of methane and some silicone polymers, boiled off and was pyrolized to the carbon and silicon noted in the spectra. This mechanism seems justified in view of the fact that Sylgard has a rather low heat of vaporization.

The powdered ablator material was changed in appearance considerably after being subjected to the hyperthermal environment behind the reflected shock. The particles changed in color from a white before the run to a gray afterward. The ablator residue became darker as the temperature was increased in the shock tube. The particles were also much smaller and did not tend to stick together as they did originally. The change in the color of the residue was probably due to a more complete breakdown of the polymer.

XII. CONCLUDING REMARKS

The luminosity resulting from a shock excited ablator material was investigated spectrographically to determine the products of ablation. The ablating material tested was a silicone polymer Sylgard 182 which has the form

$$\left[\begin{array}{c} CH_3 \\ | \\ Si - O \\ | \\ CH_3 \end{array}\right]_n$$

The powder ablator material was exposed to the high temperatures behind a reflected shock in a buffered shock tube. The temperature range investigated was from 5000° K to 10,000° K. The resultant radiation was viewed in the near ultraviolet and visible regions of the spectrum from 2400 Å to 6600 Å.

The only products of ablation which produced sufficient luminosity to be seen on the spectrographic plates were C I, SiI, and C_2. At the lower temperatures tested, the C_2 Swan band was the most apparent. As the temperature was increased, the relative intensity of the SiI lines increased. The intensity of the C_2 Swan bands decreased with increasing temperature in agreement with the theoretical equilibrium composition of the ablator material in an inert argon atmosphere at a high temperature. At the highest temperature range studied, the C I line appeared.

This investigation has shown that the technique of shock excitation of a powdered solid can be applied to the study of ablator materials. This technique can be used effectively to determine the products of ablation of a particular material in a high temperature environment.

XIII. ACKNOWLEDGMENTS

The author wishes to thank Dr. H. Y. Loh and Professor H. D. Ussery for their supervision during the course of the research and the preparation of the thesis. The help, advice, and leadership of Mr. Jim Jones and Mr. Robert Trimpi are gratefully acknowledged. The assistance of the many other people who aided in this investigation is greatly appreciated. The author also wishes to thank the secretaries for their preparation of the manuscript, those who aided in the preparation of the figures, and the laboratory technicians who aided in the research operations. The author also wishes to express his gratitude to his wife for her inspiration and patience.

XIV. BIBLIOGRAPHY

1. Ames Research Staff: Equations, Tables, and Charts for Compressible Flow. NACA Rep. 1135, 1953.

2. Arave, R. J.: Aerothermodynamic Properties of High Temperature Argon. Boeing Document No. D2-11238, 1962.

3. Breeze, J. C., and Ferriso, C. C.: Shock-Wave Integrated Intensity Measurements of the 2.7 Micron CO_2 Band Between 1200° and 3000° K. J. Chem. Phys., vol. 39, p. 2619, 1963.

4. Cambell, C. E., and Johnson, I.: Flash Spectroscopy of Radicals in the Shock Tube. J. Chem. Phys., vol. 27, p. 316, 1957.

5. Clouston, A. G., Gaydon, A. G., and Glass, I. I.: Temperature Measurement of Shock Waves by the Spectrum Line Reversal Method. Proc. Roy. Soc., vol. 248, p. 429, 1958.

6. Doherty, L. R.: The Measurement of Absolute Spectral Line Strengths With the Shock Tube. University of Michigan PhD Dissertation, 1962.

7. Eschenroeder, A. Q., and Daiber, J. W.: Nonequilibrium Ionization in a Shock Tunnel Flow. ARS Journal, vol. 31, no. 1, p. 94, January 1961.

8. Fairbairn, A. R., and Gaydon, A. G.: Comparison of the Spectra Produced by Shock Waves, Flames, and Detonations. Nature, vol. 175, p. 253, 1955.

9. Fairbairn, A. R., and Gaydon, A. G.: Spectra Produced by Shock Waves, Flames, and Detonations. Proc. Roy. Soc. London, vol. 239, p. 464, 1957.

10. Ferri, A., ed.: Fundamental Data Obtained From Shock-Tube Experiments. AGARDograph No. 41, Pergamon Press, 1961.

11. Glass, I. I., and Hall, J. G.: Shock Tubes. University of Toronto Institute of Aerophysics Review No. 12, May 1958.

12. Hertzberg, A., Smith, W. E., Glick, H. S., and Squire, W.: Modifications of the Shock Tube for the Generation of Hypersonic Flow. CAL Report No. AD-789-A-2, AEDC TN 55-15, AD 56190, March 1955.

13. Hertzberg, G.: Molecular Spectra and Molecular Structure, I. Spectra of Diatomic Molecules. D. Van Nostrand Company, Inc., 1950.

14. Keck, J., Camm, J. I., and Kivel, B.: Absolute Emission Intensity of Schumann-Runge Radiation From Shock Heated Oxygen. J. Chem. Phys., vol. 28, p. 723, 1958.

15. Keck, J., Camm, J. I., Kivel, B., and Wentink, R., Jr.: Radiation From Hot Air, Part II, Shock Tube Study of Absolute Intensities. Annals of Physics, vol. 7, pp. 1-38, 1959.

16. Laporte, O., and Wilkerson, T. D.: Hydrodynamic Aspects of Shock Tube Spectroscopy. Journal of the Optical Society of America, vol. 50, p. 1293, 1960.

17. Lapp, M.: Shock Tube Measurements of the f-Number for the (0,0)-Band of the $OH\ ^2\Sigma \rightarrow {}^2\Pi$ Transitions. J. Quant. Spectrosc. Radiant Transfer, vol. 1, p. 30, 1960.

18. Lapworth, K. C.: Preliminary Spectrographic Measurements. NPL/Aero/380, 1959.

19. Mark, H.: The Interaction of a Reflected Shock Wave With the Boundary Layer in a Shock Tube. NACA TN 1418, 1958.

20. Meggers, W. F., Corless, C. H., and Scribner, B. F.: Tables of Spectral-Line Intensities, NBS Monograph 32, Parts I and II, 1961.

21. MIT Wavelength Tables. John Wiley and Sons, Inc., New York, 1939.

22. Moore, C. E.: A Multiplet Table of Astrophysical Interest. Revised edition. Princeton Observatory Contribution No. 20, 1945.

23. Nicholls, R. W., Parkinson, W. H., and Reeves, E. M.: The Spectroscopy of Shock-Excited Powdered Solids. Appl. Opt., vol. 2, p. 919, 1963.

24. Parkinson, W. H.: Time Resolved Absorption Studies in a Shock Tube: A New Band System of BaO. Proc. Phys. Soc., vol. 78, p. 705, 1961.

25. Parkinson, W. H., and Nicholls, R. W.: Shock Tube Spectroscopy, I. The Shock Excitation of Powdered Solids. Scientific Report No. 1, AF 19(604)-4560, 1959.

26. Parkinson, W. H., and Nicholls, R. W.: Shock Tube Spectroscopy, II. Spectroscopic Temperature and Intensity Measurements in a Shock Tube. Scientific Report No. 3, AF 19(604)-4560.

27. Parkinson, W. H., and Nicholls, R. W.: Spectroscopic Temperature Measurement in a Shock Tube Using CN as a Thermometric Molecule. Can. J. Phys., vol. 38, p. 715, 1960.

28. Parkinson, W. H., and Reeves, E. M.: Shock Tube Spectroscopy in the Ultraviolet NOM$_1$-1866-(44) NR number 012-208, 1962.

29. Pearse, R. W. B., and Gaydon, A. G.: The Identification of Molecular Spectra. Third edition, Chapman and Hall, LTD, London, 1963.

30. Petschek, H. E., Rose, P. H., Glick, H. S., Kane, A., and Kantrowitz, A.: Spectroscopic Studies of Highly Ionized Argon Produced by Shock Waves. J. Appl. Phys., vol. 26, p. 83, 1955.

31. Russo, A. L., and Hertzberg, A.: Modifications of the Basic Shock Tube to Improve Its Performance. CAL Report No. AD-1052-A-7, 1958.

32. Shackleford, W. L.: Preliminary Studies on the Spectrum of TiI Emitted Behind Reflected Shock Waves in Ti Cl_4 - Ar Mixtures. AFOSR 1738, Technical Report No. 5, AF 49(638)-984, December 1961.

33. Squire, W., Hertzberg, A., and Smith, W. E.: Real Gas Effects in a Hypersonic Shock Tunnel. CAL Report No. AD-789-A-1, AEDC-TN 55-14, AD 56189, March 1955.

34. Turner, E. B.: The Production of Very High Temperatures in the Shock Tube With an Application to the Study of Spectral Line Broadening. Technical Report AFOSR TN 56-150, AD 86309, May 1956.

35. Williamson, T. D.: The Use of the Shock Tube as a Spectroscopic Source With an Application to the Measurement of gf-Values for the Lines of Neutral and Singly Ionized Chromium. University of Michigan PhD Dissertation, June 1961.

36. Wilson, M. R., and Wittliff, C. E.: Low-Density Stagnation Point Heat Transfer Measurements in the Hypersonic Shock Tunnel. ARS Journal, vol. 32, no. 2, p. 275, February 1962.

37. Wright, J. K.: Shock Tubes. Methuen's Monographs on Physical Subjects, 1961.

38. Wurster, W. H., and Glick, H. S.: Ultraviolet Spectrum of Air at 5750° K. J. Chem. Phys., vol. 28, p. 1218, 1957.

39. Wurster, W. H., Click, H. S., and Treanor, C. E.: QM-997-A-1, Cornell Aeronautical Laboratory, Buffalo, New York, 1957.

40. Zeleznik, F. J., and Gordon, S.: A General IBM 704 or 7090 Computer Program for Computation of Chemical Equilibrium Compositions, Rocket Performance, and Chapman Jouget Detonations. NASA TN D-1454, 1962.

41. Zeleznik, F. J., and Gordon, S.: An Analytical Investigation of Three General Methods of Calculating Chemical-Equilibrium Compositions. NASA TN D-473, 1960.

XV. VITA

Roger D. Bengtson was born on April 29, 1941, in Wausa, Nebraska, where he attended primary and secondary schools. He attended the University of Nebraska and received a Bachelor of Science degree in 1962. Since graduation he has been with present employer, the National Aeronautics and Space Administration. Langley

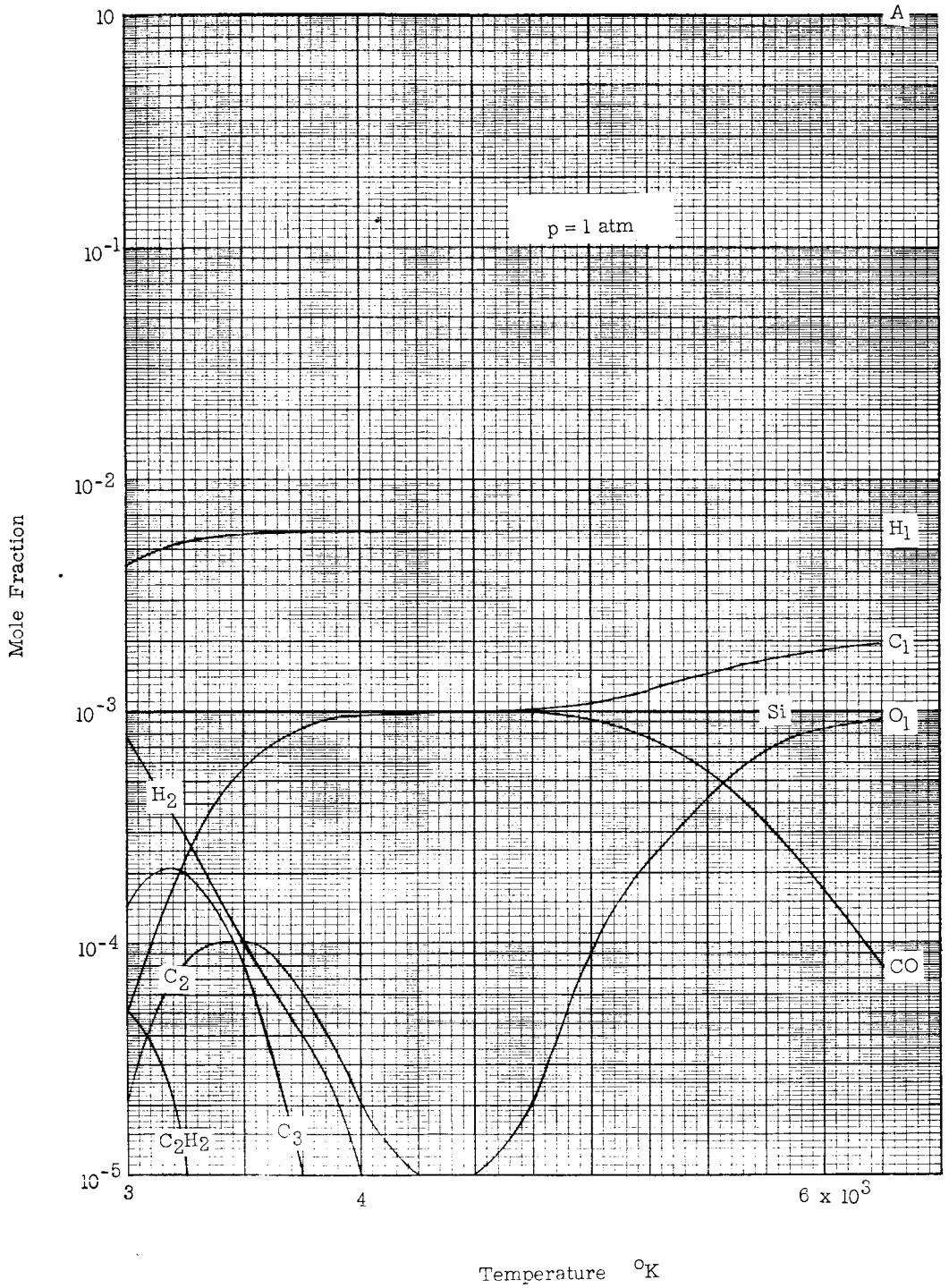

Figure 1(a).- Equilibrium gas composition of an elemental mixture of 0.99 A, 0.006 H, 0.002 carbon, 0.001 Si, and 0.001 O.

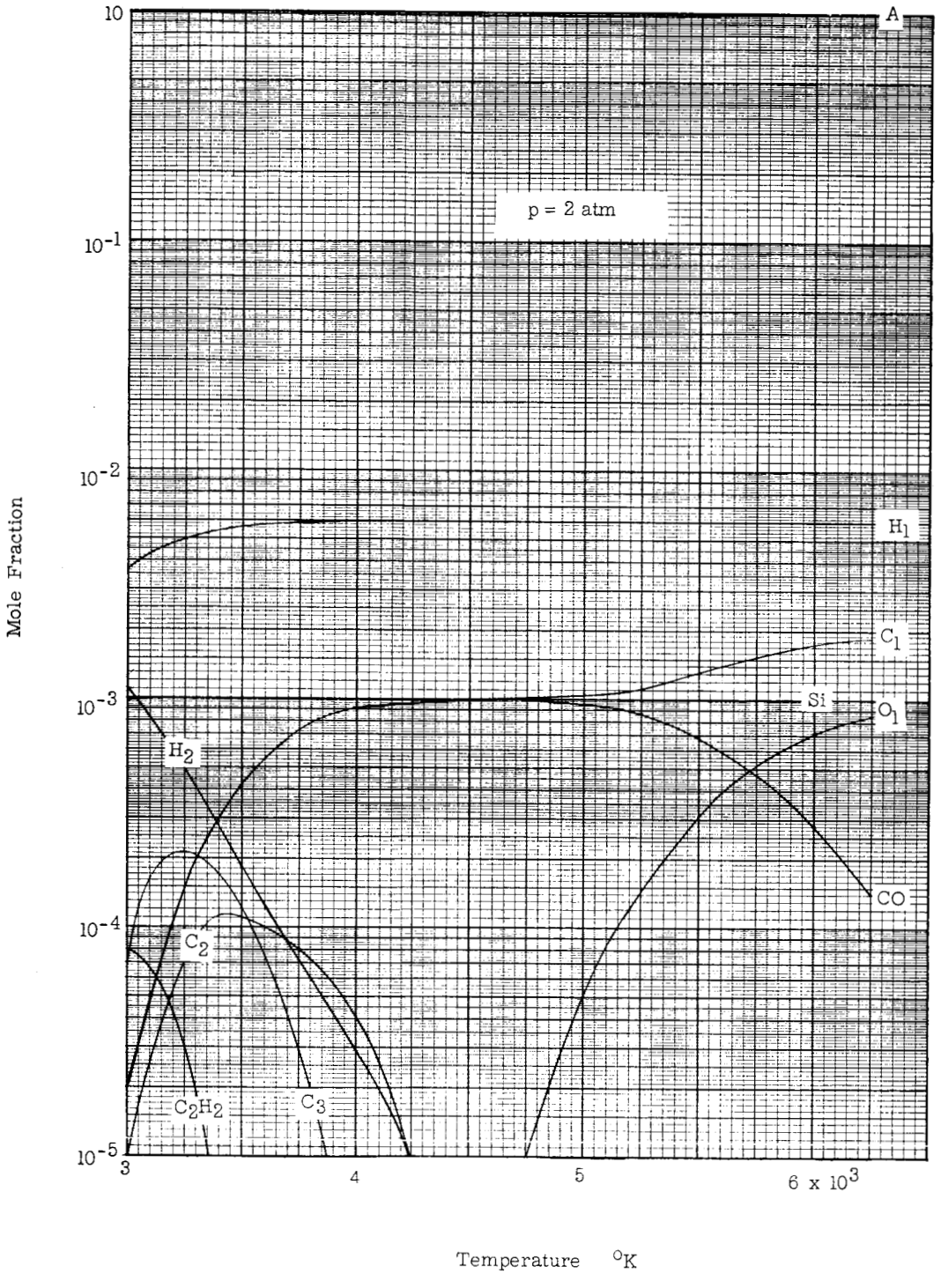

Figure 1.- Continued.

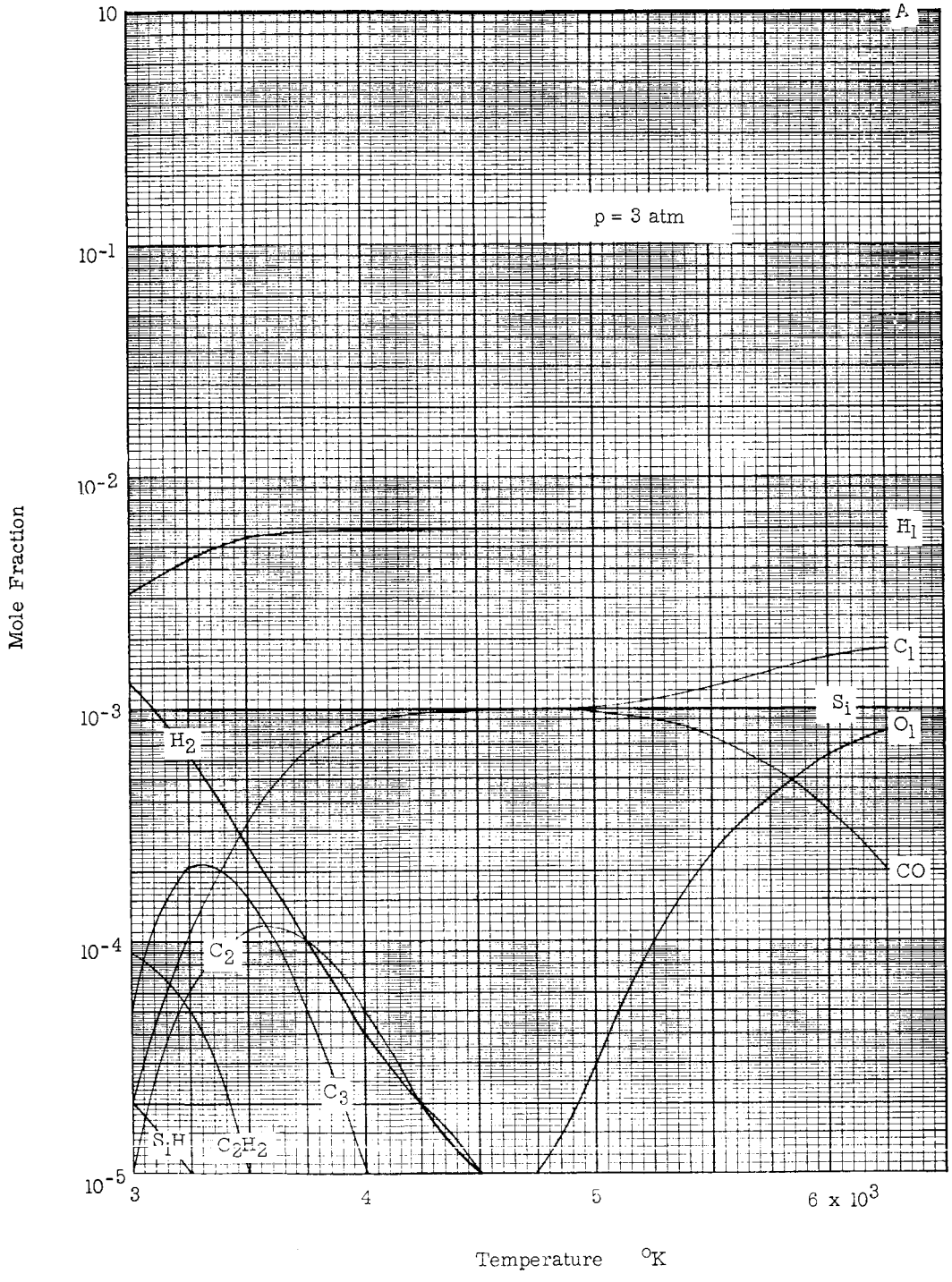

Figure 1.- Continued.

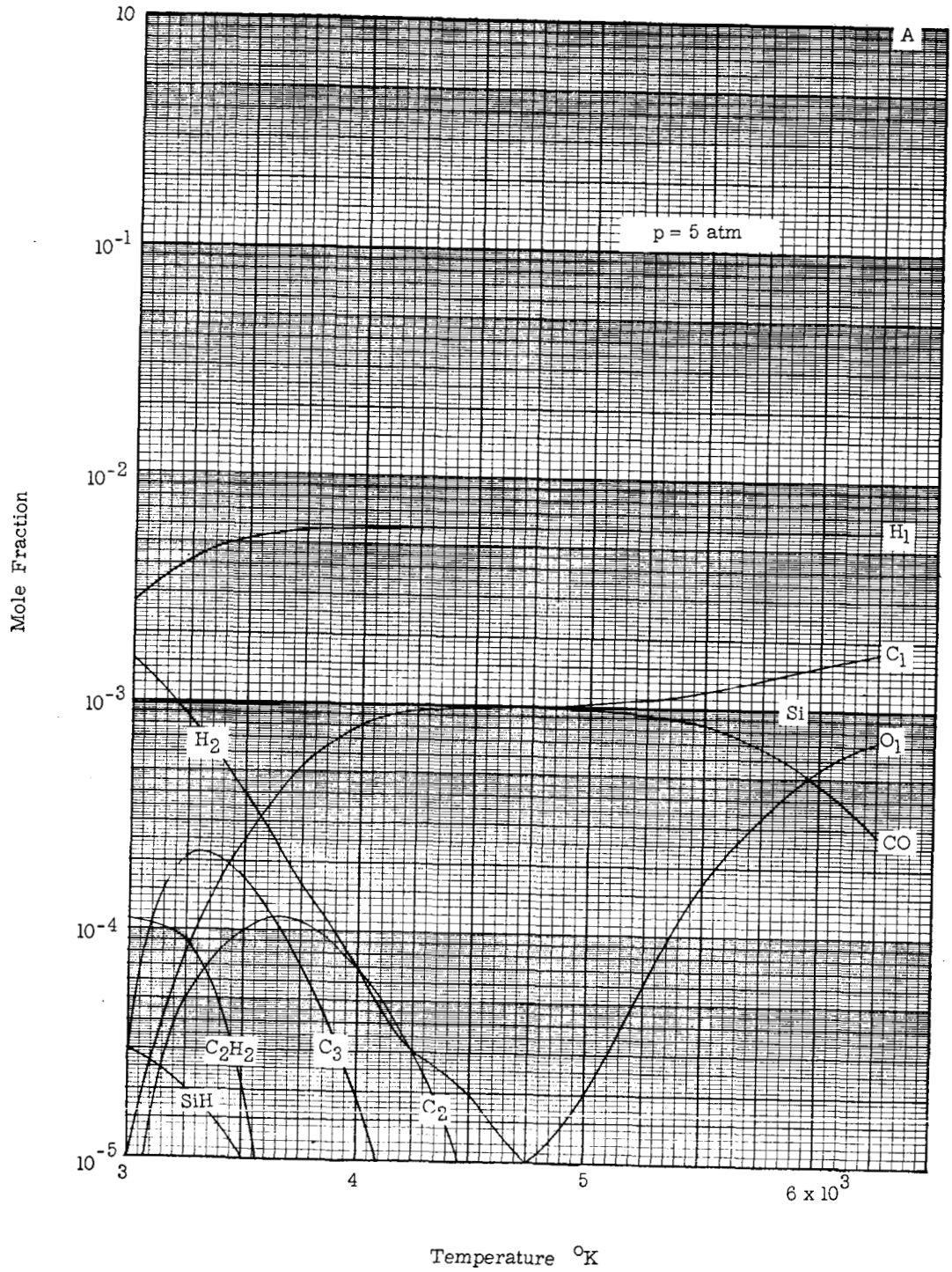

Figure 1.- Concluded.

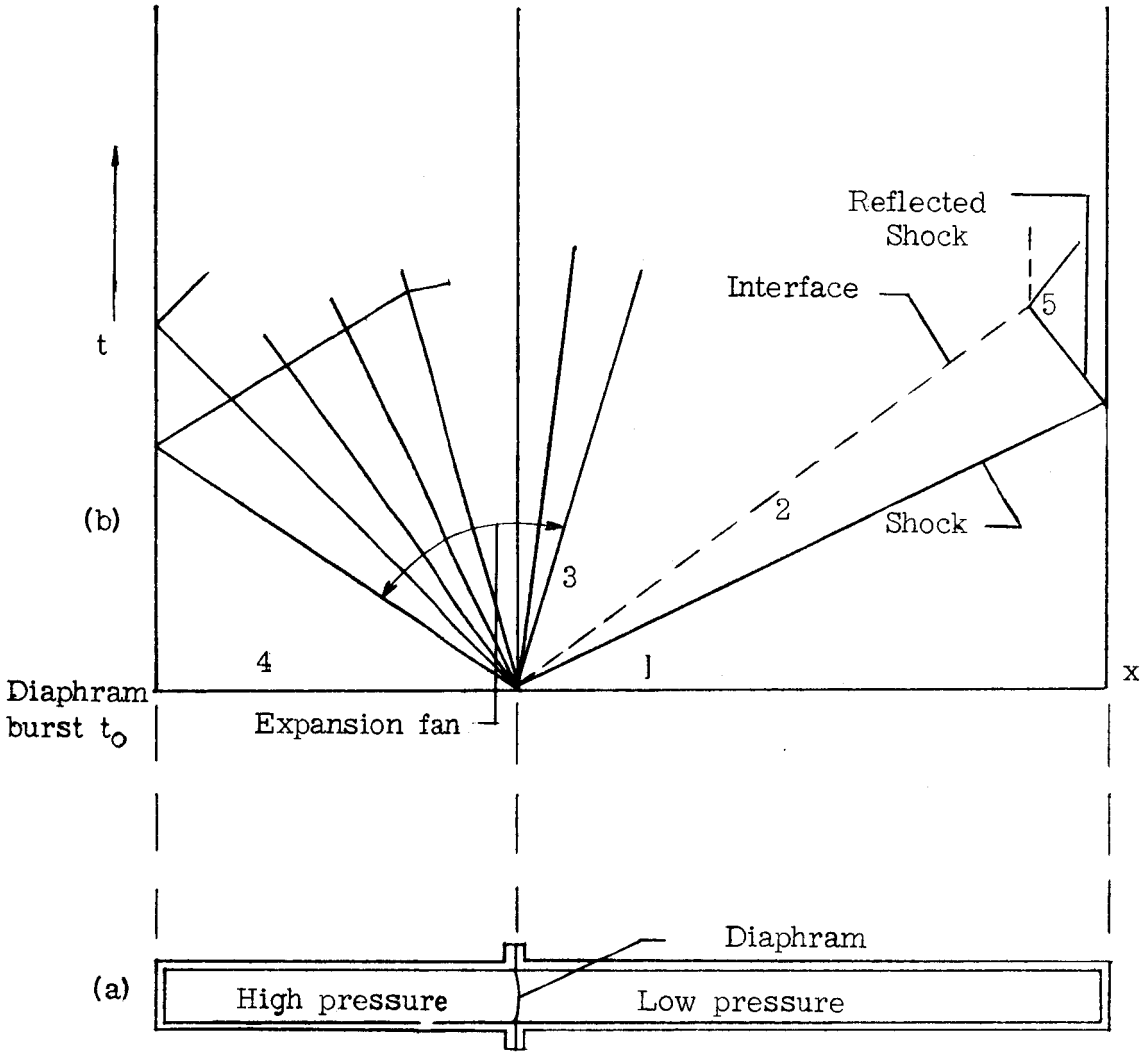

Figure 2.- Ideal wave motion in a simple shock tube.

Normal Shock Wave

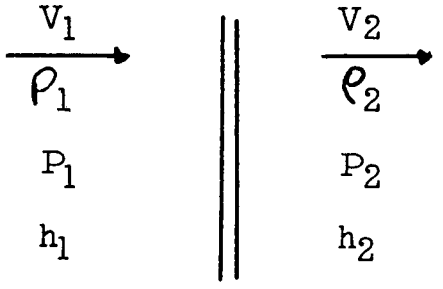

Figure 3.- Schematic of normal shock with gas parameters.

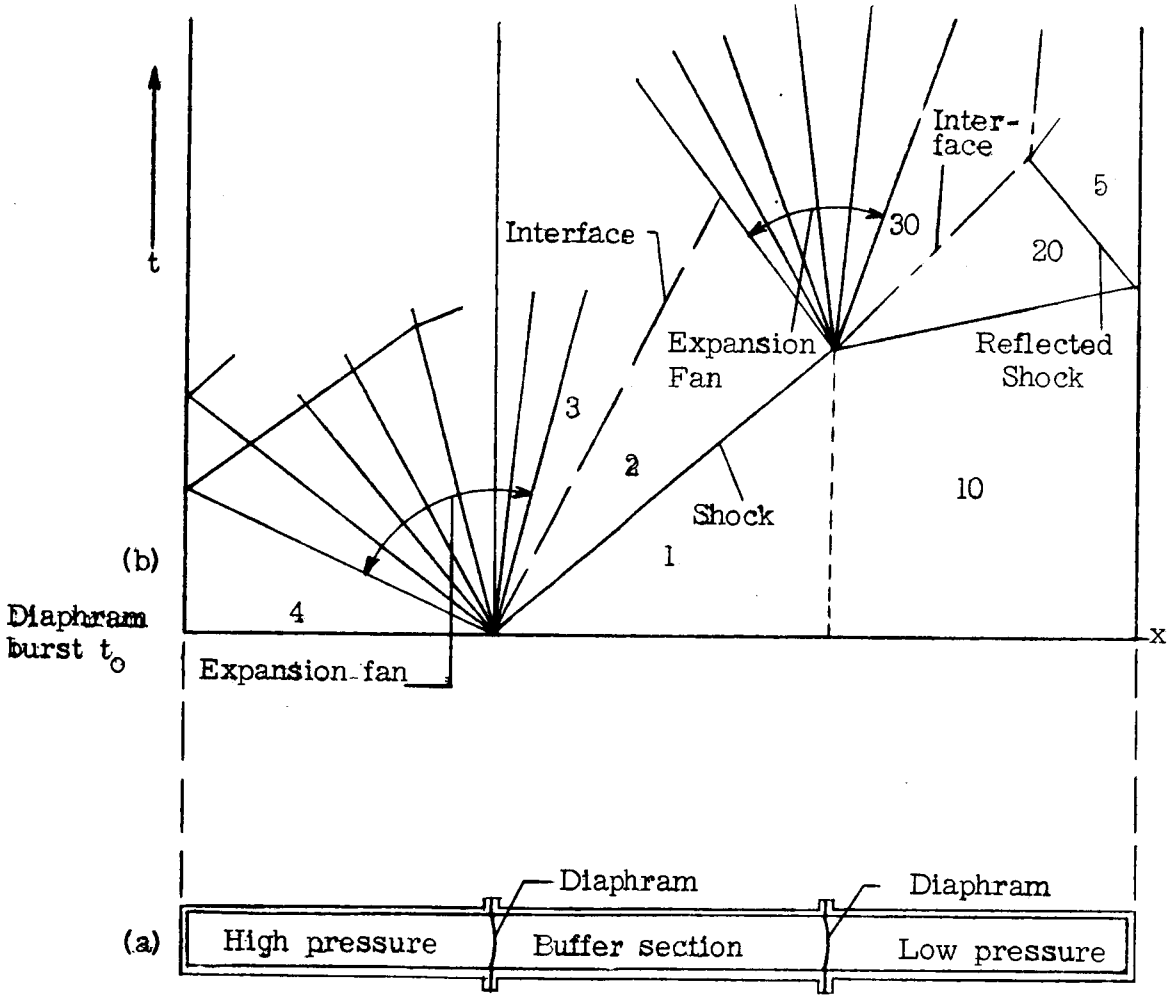

Figure 4.- Ideal wave motion in a buffered shock tube.

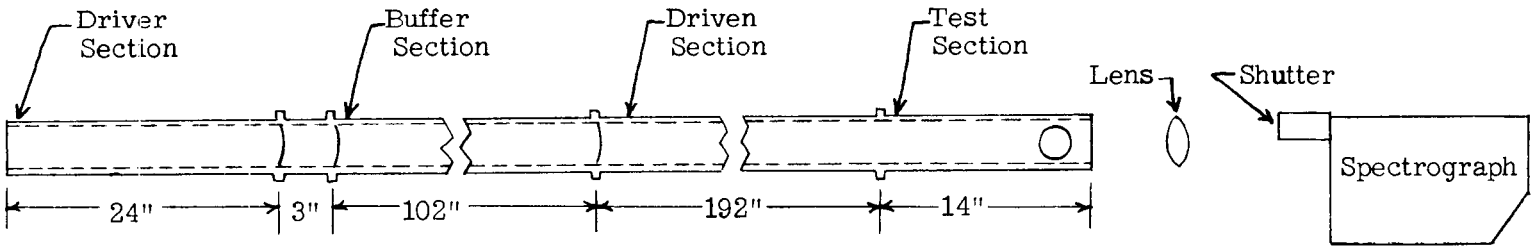

Figure 5.- Schematic of experimental apparatus.

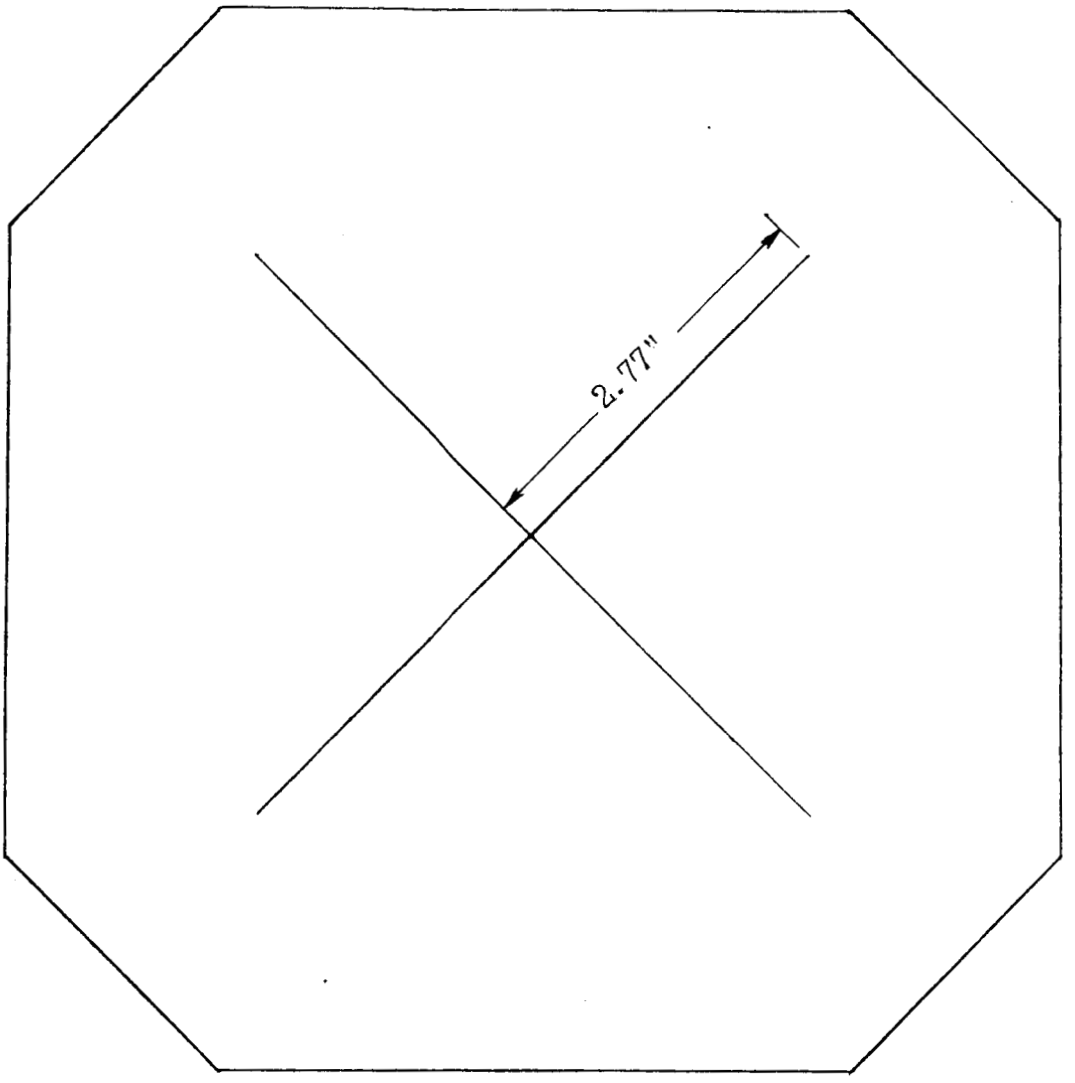

Detail of Scribe

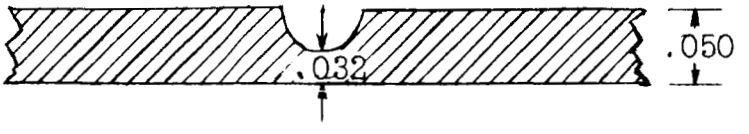

Figure 6.- Diaphragm and scribe.

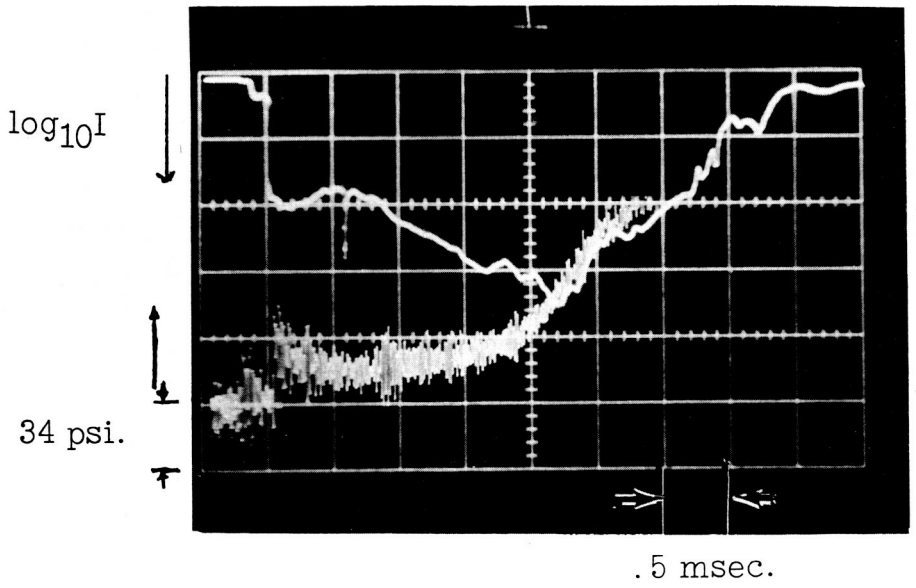

Figure 7(a).- Pressure and intensity record.

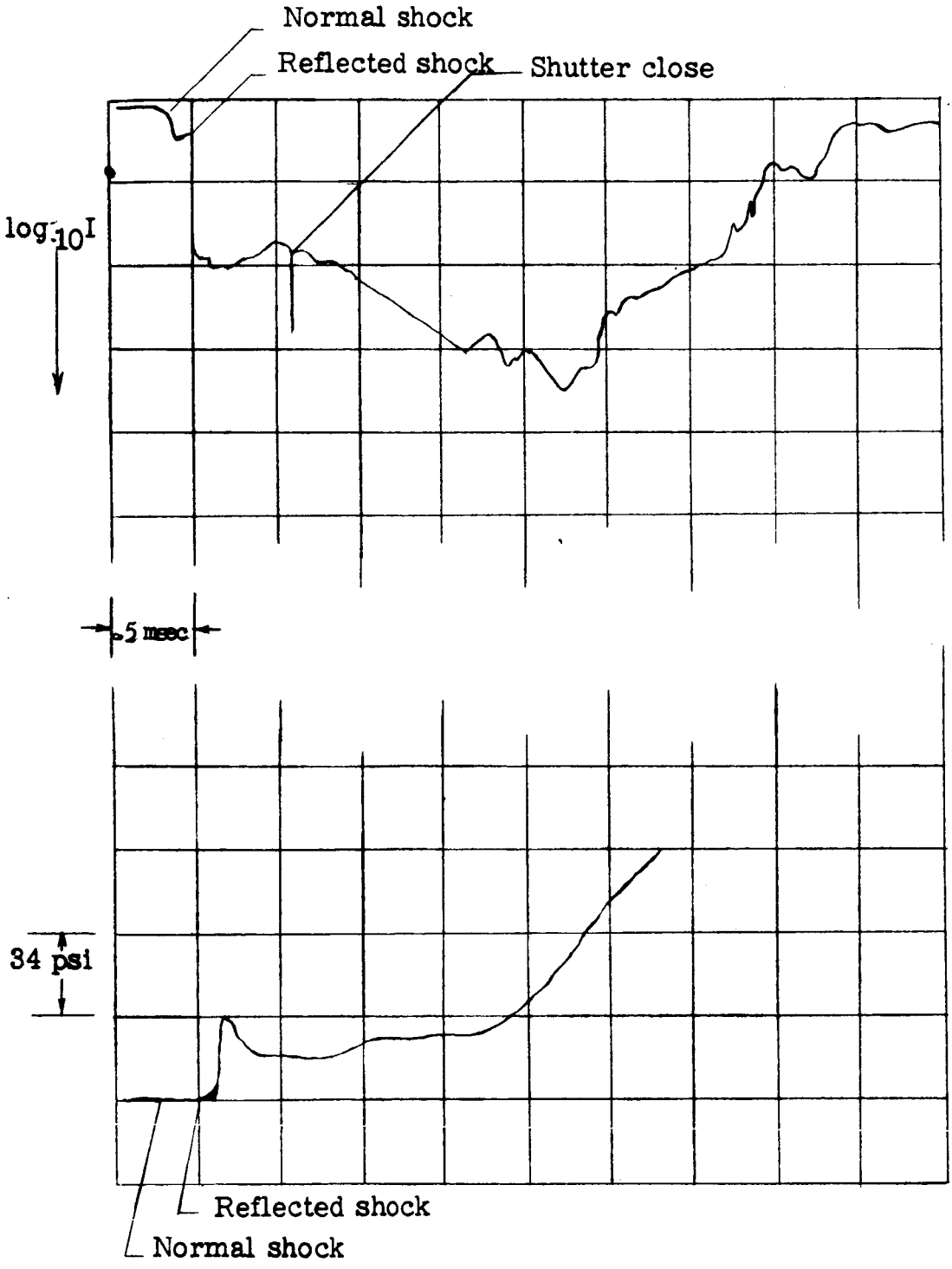

Figure 7.- Concluded.

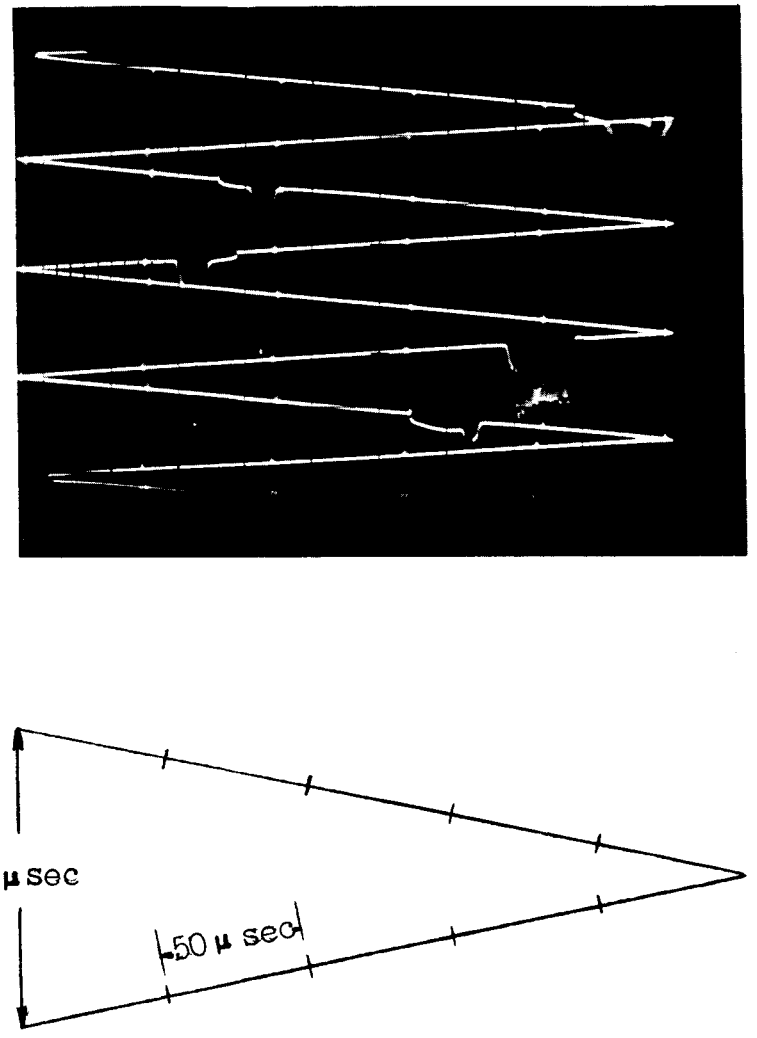

Figure 8.- Raster timer output.

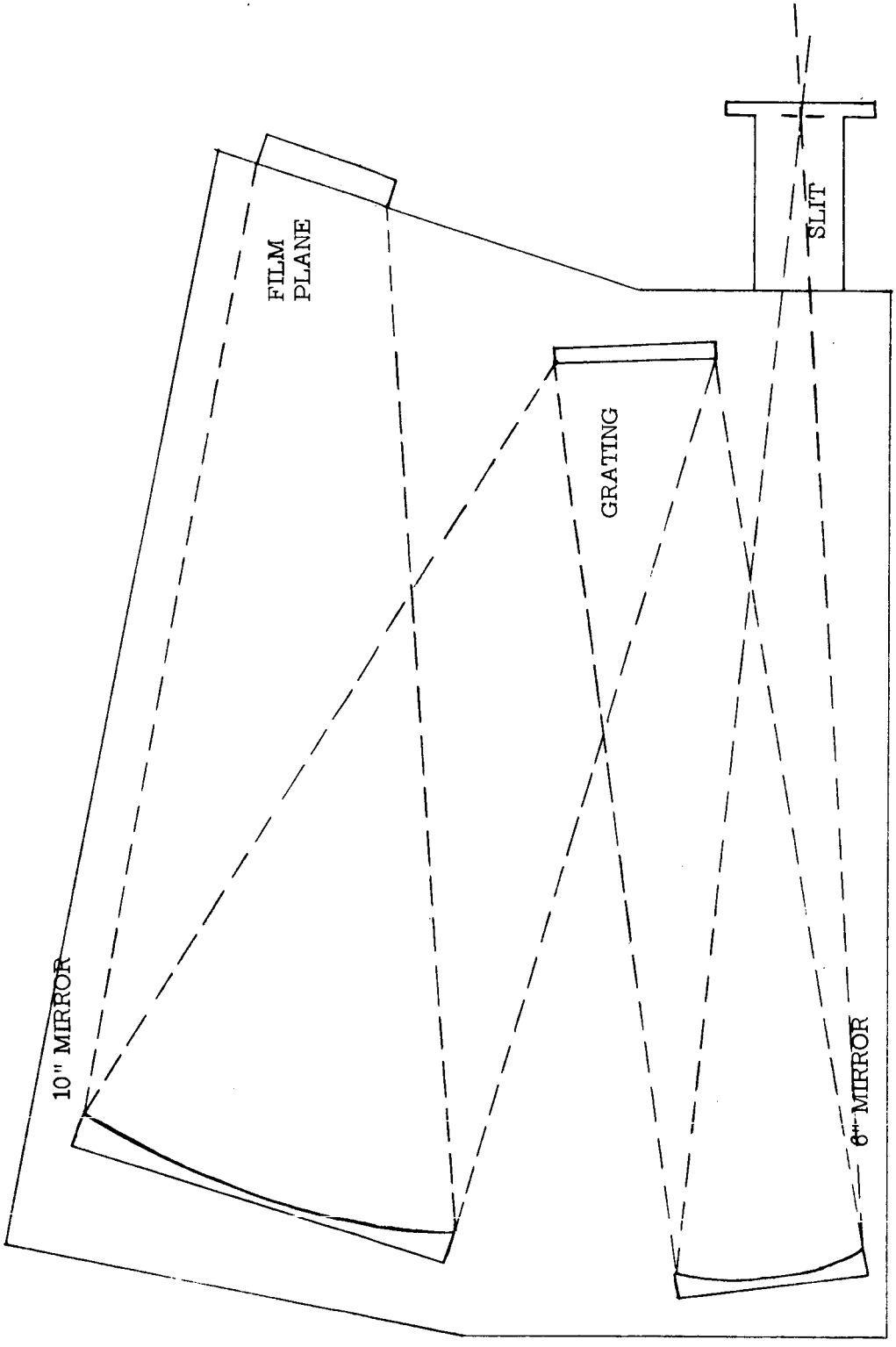

Figure 9.- Optical path of spectrograph.

No.	P_{10} mm	V_s ft/sec	M_s	T_2 °K	T_5 °K	P_5 in psi		Shutter closing time in msec	Film characteristics	Tube additive
						Measured	Calculated			
40	17	5200	4.9	2580	5700	51	53	1.5	103-0	Sylgard on Kleenex
41	18	5200	4.9	2580	5700	51	56	1.5	103-0	Sylgard on Kleenex
44	12	6670	6.3	3960	9150	31	65	1.0	103-0	Sylgard on Kleenex
51	6	7000	6.6	4320	9900	20	40	1.1	103-0	Sylgard on Kleenex
52	21	4800	4.5	2160	4950	--	57	1.1	103-0	Sylgard on Kleenex
53	10	6210	5.8	3390	7950	26	43	1.1	103-0	Sylgard on Kleenex
55	19	4960	4.7	2370	5250	--	55	1.1	103-F	Sylgard on Kleenex
58	9	5800	5.5	3090	7050	31	37	1.1	103-F	Sylgard on Kleenex
60	6	6700	6.3	3960	9150	19	32	1.1	103-F	Sylgard on Kleenex
61	12	--	---	--	--	26	--	1.1	103-F	Kleenex
70	12	6180	5.8	3390	7950	28	51	1.1	103-F	Sylgard on Kleenex

Figure 10.- Run conditions.

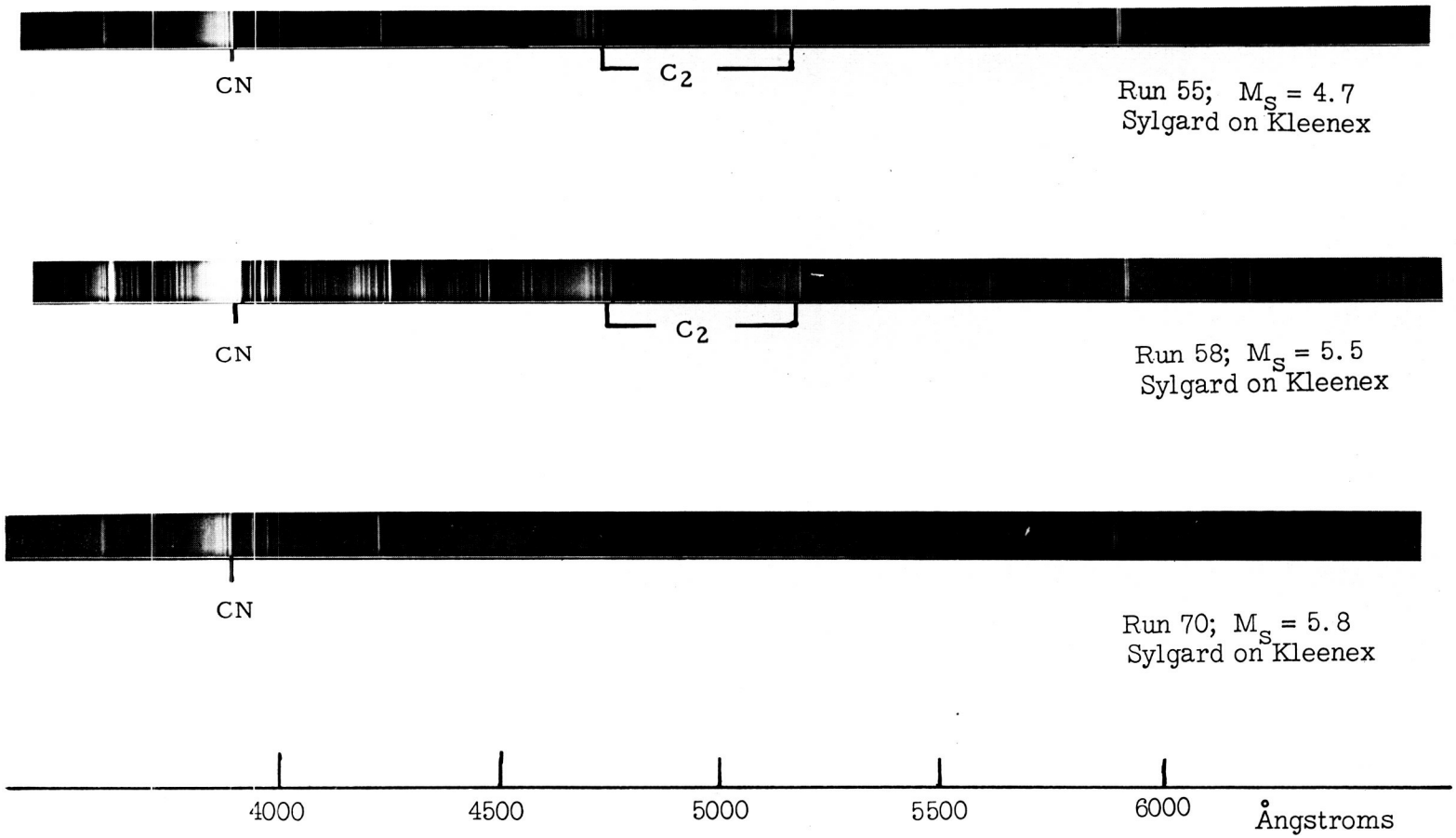

Figure 11(a).- Shock excited spectra.

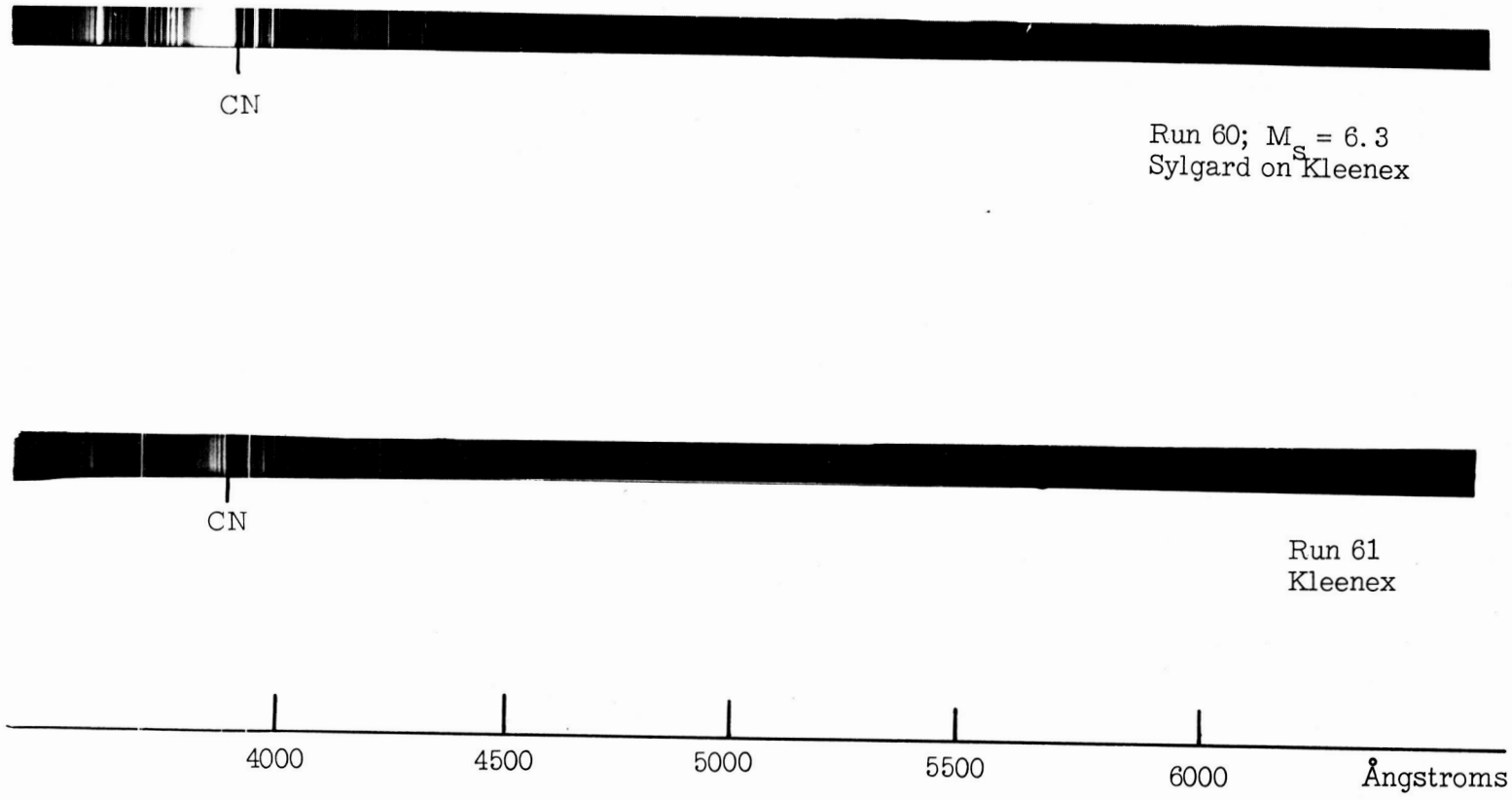

Figure 11.- Continued.

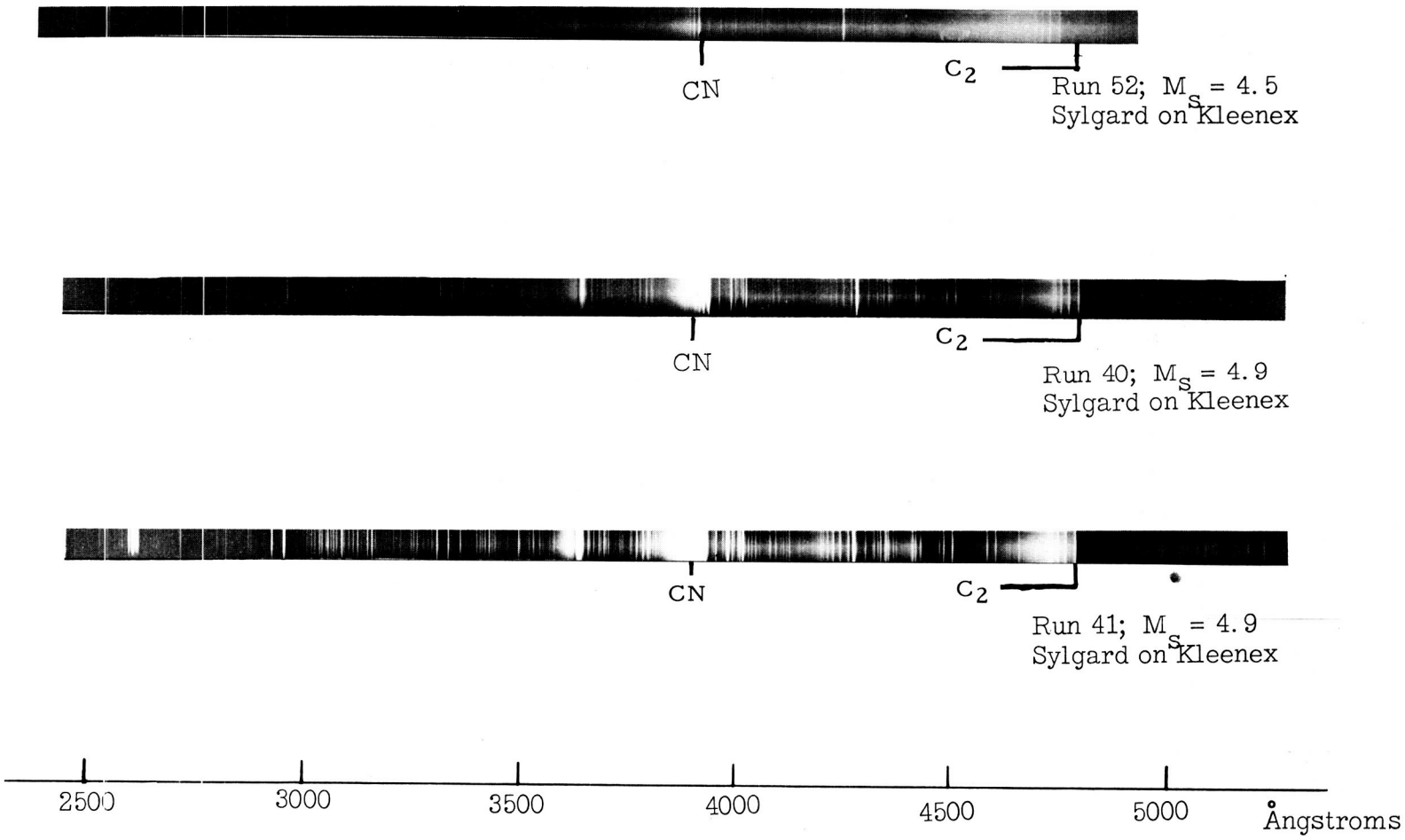

Figure 11.- Continued.

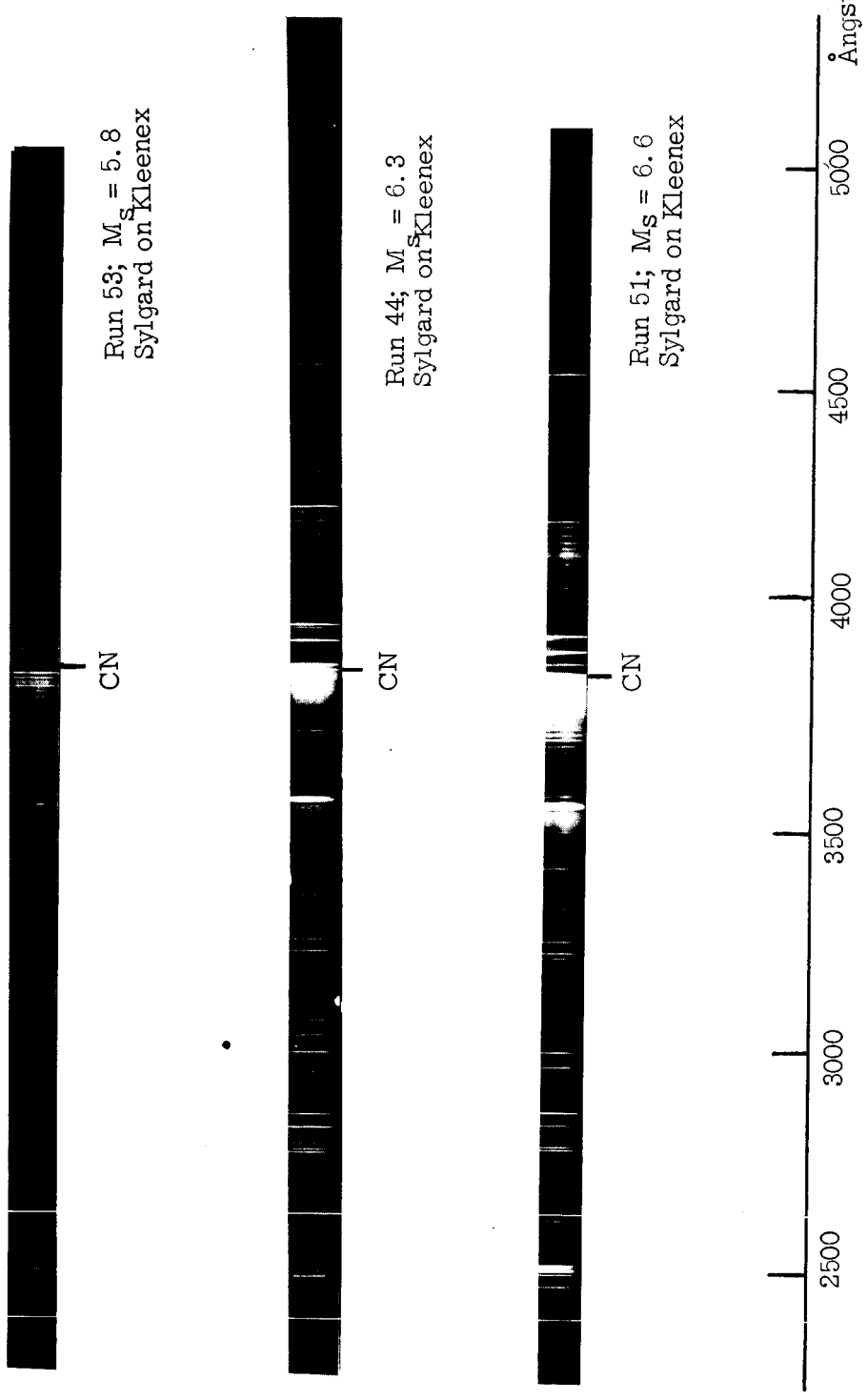

Figure 11.- Concluded.

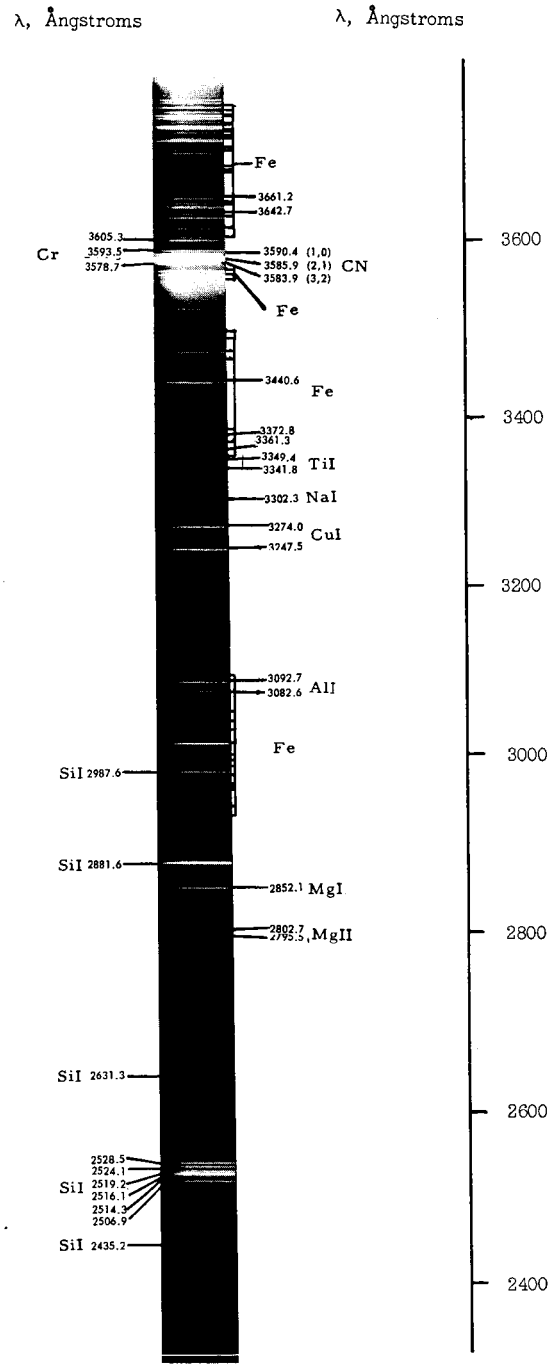

(a) Run 41.

Figure 12.- Shock excited spectra.

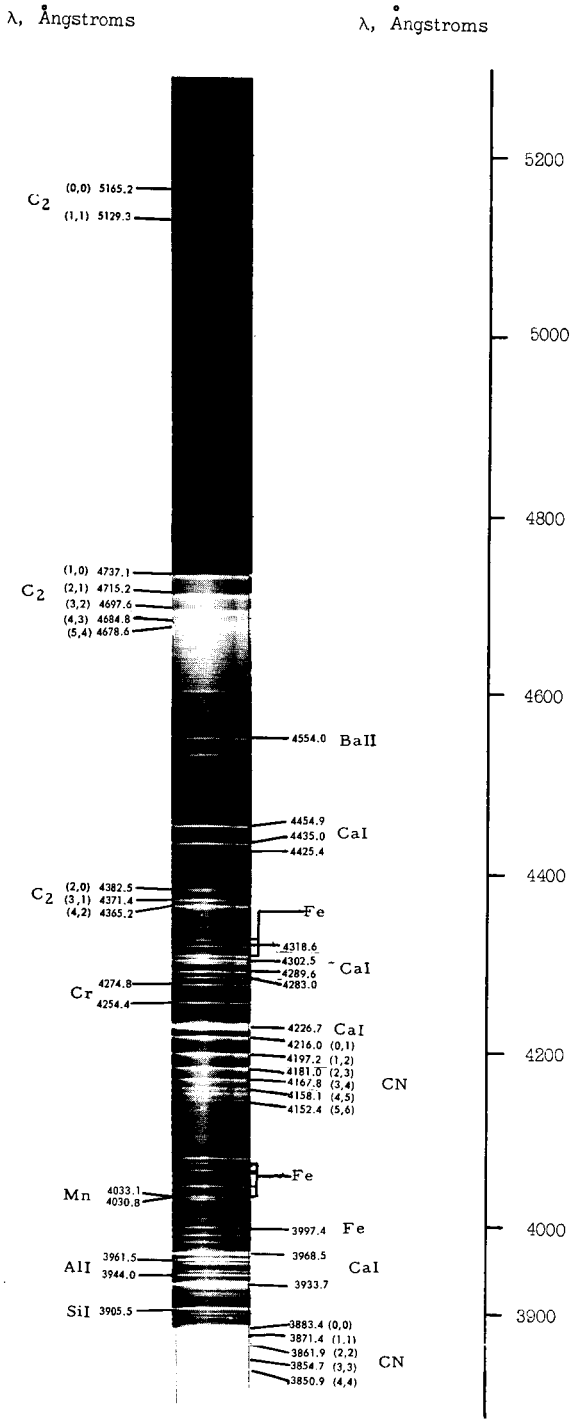

(b) Run 41.

Figure 12.- Continued.

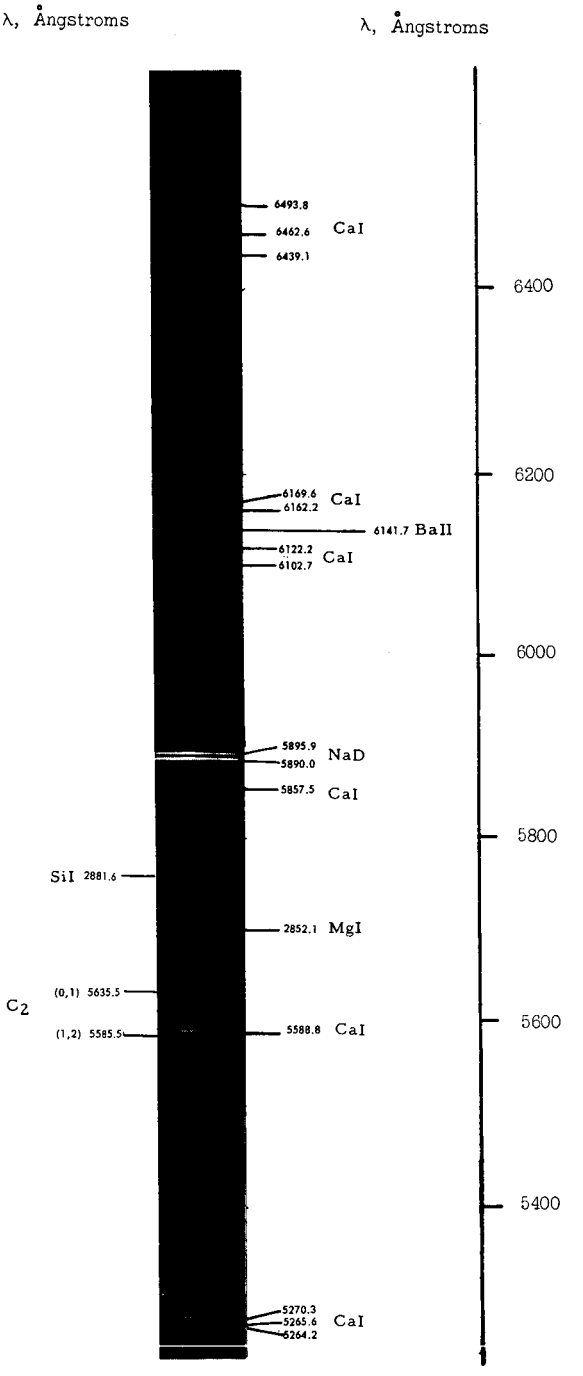

(c) Run 58.

Figure 12.- Concluded.

SPECTROGRAPHIC INVESTIGATION OF A SHOCK EXCITED ABLATION MATERIAL

By

Roger D. Bengtson

ABSTRACT

The radiation resulting from a shock heated powdered ablator material was investigated spectrographically to determine the products of ablation. The ablating material tested was a silicone polymer, Sylgard 182, manufactured by Dow Corning, which has the form

$$\left[\begin{array}{c} CH_3 \\ | \\ Si - O \\ | \\ CH_3 \end{array}\right]_n$$

The powdered ablator material was exposed to the high temperature behind the reflected shock in a buffered shock tube. The temperature range investigated was from 5,000° K to 10,000° K. The resultant radiation was viewed in the near ultraviolet and visible regions of the spectrum from 2,400 Å to 6,600 Å. The only products of ablation that produced sufficient luminosity to be seen on the spectrographic plates were C I, SiI, and C_2. An analytic investigation was also carried out which determined the equilibrium chemical composition of a mixture of gases found in a typical shock tube run behind the reflected shock.